

**MRI IMAGING APPEARANCE IN MULLERIAN DUCT ANOMALIES.*****Yasmin Tharwat Elsaed Elsaed, Naglaa Hussein Shebrey, Samar Ramzy Ragheb.*****ABSTRACT:**

Radiology department, faculty of medicine, Ain Shams university, Cairo, Egypt.

**Corresponding author:**

Yasmin Tharwat Elsaed Elsaed

Mobile: +20 01024055359

e.mail: :

[yasmin\\_2014@hotmail.com](mailto:yasmin_2014@hotmail.com)

Received: 16/2/2023

Accepted: 8/3/2023

**Online ISSN: 2735-3540**

**Background:** Müllerian duct anomalies include a complex spectrum of anatomical anomalies that arise from deviations during the normal development of the Müllerian ducts. In paediatrics, such defects cannot present with any clinical symptoms before puberty, yet, they can also have obstructive symptoms or a mass effect due to presence of a non-communicating rudimentary horn or transverse vaginal septum. At the beginning of puberty, girls with these anomalies might have primary amenorrhea, pelvic pain or endometriosis. Müllerian duct anomalies have also associated with a variety of other congenital abnormalities.

**Aim of the work:** To review MRI features of Mullerian Duct Anomalies and classify them according to American Fertility Society and American Society of Reproductive Medicine (AFS/ASRM) and the European Society for Human Reproduction and Embryology (ESHRE) and European Society for Gynecological Endoscopy (ESGE) classifications.

**Patients and Methods:** The study was a case series study that included 37 patients who underwent pelvic MRI at Radiology Department "Ain Shams University hospitals" in Cairo, Egypt. MRI features of Mullerian duct anomalies were reviewed and classified according to the AFS/ASRM and the ESHRE/ESGE classifications.

**Results:** According to AFS/ASRM, uterine anomalies were categorized as none (unclassified) in 2 patients, class 1 (agenesis) in 16 patients, class 2 (unicornuate) in 2 patients, class 3 (didelphys) in 8 patients, class 4 (bicornuate) in 5 patients, class 5 (septate) in 3 patients and class 6 (arcuate) in 1 patient. According to ESHRE/ESGE, the uterus was 0 (normal) in 2 patients, 1 (dysmorphic) in 9 patients, 2 (septate) in 3 patients, 3 (bicorporeal) in 13 patients, 4 (hemi-uterus) in 2 patients and 5 (aplastic) in 8 patients. Similarly, the cervix was 0 (normal) in 17 patients, 2 (double) in 8 patients and 4 (aplastic) in 12 patients and the vagina was 0 (normal) in 16 patients, 1(longitudinal non obstructing vaginal septum) in 1 patient, 2 (longitudinal obstructing vaginal septum) in 5 patients, 3 (transverse vaginal septum) in 3 patients and 4 (aplastic) in 12 patients.

**Conclusion:** MRI is a highly helpful technique for evaluating female genital abnormalities and is able to consistently provide the essential imaging characteristics for the accurate identification of Mullerian malformations. Additionally, incidental pelvic disease and any related renal abnormalities may be thoroughly evaluated by MRI in a single scan, removing the need for additional diagnostic procedures.

**Keywords:** Mullerian duct anomalies, MRI, American Fertility Society and American Society of Reproductive Medicine (AFS/ASRM) and the European Society for Human Reproduction and Embryology

## **INTRODUCTION:**

Müllerian Duct Anomalies are due to abnormal development and fusion, or cannalization of the Müllerian duct system throughout embryogenesis<sup>(1)</sup>, which give rise to the uterus, cervix, upper two thirds of the vagina, and fallopian tubes. The lower third of the vagina and ovaries are not influenced by Mullerian Duct Anomalies as they develop in distinct embryologic paths. Although the certain cause of these anomalies is unclear, recent research refer to both environmental and inherited causes<sup>(2)</sup>.

It is unclear how common Mullerian duct abnormalities are, as many patients are asymptomatic. Other cases may develop amenorrhea, endometriosis, or pelvic pain at onset of puberty together with secondary sexual characteristics that are typically normal. The only sign of müllerian abnormal development in adult women may be infertility or poor reproductive consequences<sup>(3)</sup>.

Although predicts of MDA prevalence range from 0.1 to 7% of newborn, data among different communities vary greatly<sup>(3)</sup>, the application of variable diagnostic approaches by variable healthcare providers and the analysis of distinct patient populations can at least in part illustrate this difference. MDAs are generally accepted to be present in 13.3-16.7% of patients who experience repeated miscarriages, 4-8.0% of infertile women, and 24.5% of patients who experience both infertility and miscarriage<sup>(3)</sup>.

The prevalence of Mullerian tube anomalies in Egypt is about 18% of all congenital malformations<sup>(4)</sup>. For the first evaluation of Müllerian duct abnormalities, ultrasound (US) is usually used as the first modality; even so. US is insufficient for the detailed characterisation of the anomaly<sup>(5)</sup>.

The uterovaginal anatomy may be seen in great detail using magnetic resonance imaging. It can also be utilised to determine the uterus' size and if the rudimentary horns contain active endometrial tissue or not. Magnetic resonance imaging can also be used to determine the shape and position of the ovary, as well as any additional possible complications such obstruction, endometriosis, or related kidney anomalies<sup>(3)</sup>.

MRI is not affected by body habit or underlying intestinal gas, unlike ultrasound. Hysterosalpingography uses ionising radiation, which should be avoided whenever possible in young patients, whereas MRI does not use the ionising radiation and also is non-invasive. Both transvaginal pelvic sonography and hysterosalpingography require vaginal examination which make them less tolerable in children than in adults<sup>(6)</sup>.

Together, these elements have made MRI the "gold standard" imaging modality, as it has been demonstrated to be exceptionally accurate in the diagnosis of MDA and it has replaced earlier techniques<sup>(6)</sup>. Laparoscopic confirmation is rarely necessary for uterine abnormalities due to the excellent accuracy of MRI in the diagnosis<sup>(7)</sup>.

The American Fertility Society and American Society of Reproductive Medicine (AFS/ASRM) approved a classification system for Müllerian abnormalities in 1980 with only minor adjustments<sup>(8)</sup>. The ASRM classification system has been successfully utilised as the main categorization method for more than 20 years since it is straightforward and sufficiently clear. But this classification has a number of limitations, including the inability to accurately identify a variety of congenital abnormalities into the main categories and subcategories of

the ASRM system. The newest classification system for Mullerian duct anomalies, developed by the European Society for Human Reproduction and Embryology (ESHRE) and European Society for Gynecological Endoscopy (ESGE) is more accommodative than the ASRM classification<sup>(9)</sup>.

---

**AIM OF THE WORK:**

To review MRI features of Mullerian Duct Anomalies and classify them according to American Fertility Society and American Society of Reproductive Medicine (AFS/ASRM) and the European Society for Human Reproduction and Embryology (ESHRE) and European Society for Gynecological Endoscopy (ESGE) classifications.

---

**PATIENTS AND METHODS:**

The current study was conducted at Ain Shams University from March 2021 to September 2021, in which thirty-seven patients were included. The inclusion criteria contained primary amenorrhea, severe

dysmenorrhea, repeated miscarriage or infertility showed abnormal gynaecological ultrasonography or abnormal hysterosalpingography. Whereas the excluded patients were those patients who suffer from claustrophobia, patients with known contraindications for MRI examinations, e.g. pacemakers, and aneurysm clip and patient treated with chemotherapy.

The patients had MR examination using a 1.5 T machine (Achieva and Ingenia, Philips medical system, Eindhoven, Netherlands) with phased-array MR surface coil. ASRM and the most recent classification ESHRE/ESGE of congenital anomalies of the female genital tract was used for the description of abnormal findings. Parameters of MR sequences included sagittal T2-weighted fast spin-echo sequence from one femoral head to the other, oblique axial (perpendicular to the long axis of the uterus) T1- weighted sequence and T2-weighted fast spin-echo sequence from the renal hilum to the symphysis pubis, and oblique Coronal T2 weighted sequence (parallel to the long axis of the uterus) as shown in table (1).

**Table (1):** MRI sequences used in the study:

Sequence	TR (msec.)	TE (msec.)	FOV (mm)	Matrix	Slice thickness (mm)
T2 sagittal	3060	100	290 x290	208x 205	4
T2 axial	5210/71	100	288 x 350	292 x 180	5
T1 axial	2470/ 10	20	260 x 216	272x200	5
T1 DWI axial	1800/ 100	65	240 x 240	240 x 190	5
T2 coronal	4000/94	100	300x300	263 x 171	4.5

**Image Analysis:**

MRI images were assessed for uterus, vagina, gonads, and associated pelvic lesions and renal anomalies. Regarding the uterine size, the uterine length was measured and the uterine body to the cervix ratio was also calculated in the sagittal plane since the normal uterine length measures 6–9 cm and the uterine body to the cervix ratio is 2:1. For the inter-cornual distance (the distance between the distal ends of the horns), the

oblique long-axis views were used as it normally measures 2-4 cm. Alternatively, the external fundal contour of the uterus was most seen in long-axis oblique views as is typically convex. The inter-cornual angle (the angle between the two uterine hemi cavities' medial aspect which often falls between 75 and 105 degrees) was also measured. Similarly, the zonal anatomy, as shown in T2-weighted imaging, is the division of the high-signal-intensity

endometrium, low-intensity junctional zone (inner myometrium), and intermediate-intensity outer myometrium was also evaluated. Additionally, if a uterine septum was found, its signal intensity and extent were assessed. Blood-filled fallopian tubes (hematosalpinx) and a distended uterus (hematometra) exhibiting the distinctive signal pattern of altered blood and blood products with the level of obstruction were also determined.

The vagina was often viewed as a tube with a signal intensity that is intermediate between the bladder base and urethra up front and the anal canal down back. If there is a vaginal septum, it was evaluated for orientation and size. The obstruction site of a blood-filled vagina (hematocolpos) was also estimated. Both ovaries were identified. It was recorded if there were any associated lesions, including endometriosis or teratoma. Any related pelvic lesions or renal abnormalities that may have existed have been documented.

**Statistical Analysis:**

Data were analysed using the Statistical Package of Social Science (SPSS) program for Windows (Standard version 24). The normality of data was first tested with one-sample Kolmogorov-Smirnov test. Qualitative data were described using number and percent while continuous variables were presented as mean ± SD (standard deviation) for normally distributed data.

**Ethical Considerations:**

Our study was approved by the local ethical committee at the faculty of Medicine Ain shams University (MS 112/2021). Informed written consent was obtained from all patients.

**RESULTS:**

**Demographic data:** The mean age of patients was 23.19±8.78 years and ranged from 6 to 58 years. 7 (19.0%) patients were more than 30 years, 12 (32.4%) were less than

20 years while 18 (48.6%) are between 20-30 years as shown in Table 2.

Table (2): Demographic data of the included patients.

Age (Years)	The study group (n=37)
Age (Years) Mean ± SD Min-Max	23.19±8.78 6-58
Age categories	
<20 y	12 (32.4%)
20-30 y	18 (48.6%)
> 30 y	7 (19.0%)

**Clinical data:** Primary amenorrhea was the most common symptom representing 45.9% (17 out of 37 patients), followed by being asymptomatic in 9 patients (24.3%). Infertility was seen in 4 patients representing (10.8%). Irregular menses and abdominal pain were of the same ratio (8.1%) complained by 3 patients each, and vaginal bleeding seen in one patient representing (2.7%) as shown in Table (3).

Table (3): Distribution of presenting symptom in the included patients.

Clinical picture	The study group (n=37)
Asymptomatic	9 (24.3%)
Primary amenorrhea	17 (45.9%)
Infertility	4 (10.8%)
Irregular menses	3 (8.1%)
Abdominal pain	3 (8.1%)
Vaginal bleeding	1 (2.7%)

Concerning congenital anomalies associated with MDAs, 31 cases (83.8%) had no associations, 4 (10.8%) with absent ovaries, 1 (2.7%) with bilateral polycystic ovaries and 1 (2.7%) with left renal agenesis as demonstrated in Table (4).

Table (4): Congenital anomalies associated with MDAs in our study.

Associated anomalies	The study group (n=37)
None	31 (83.8%)
Absent ovaries	4 (10.8%)
Bilateral polycystic ovaries	1 (2.7%)
Left renal agenesis	1 (2.7%)

Uterine anomalies classification (Table 5). According to ASRM classification, there

**MRI Imaging Appearance in Mullerian Duct Anomalies.**

were 16 cases (43.2%) with uterine agenesis, 2 cases (5.4%) with unicornuate uterus, 8 cases (21.6%) with didelphys uterus, 5 cases (13.5%) bicornuate, 3 cases (8.1%) septate and 1 case (2.7%) arcuate uterus. All cases were classified according to ASRM except 2 cases (5.4%) with longitudinal vaginal septum as this system of classification does not include the cervical and vaginal anomalies.

Table (5): Uterine anomalies classification according to AFS/ASRM classification.

AFS/ASRM	The study group (n=37)
None (unclassified)	2 (5.4%)
Class 1 (Agenesis)	16 (43.2%)
Class 2 (unicornuate)	2 (5.4%)
Class 3 (Didelphys)	8 (21.6%)
Class 4 (bicornuate)	5 (13.5%)
Class 5 (septate)	3 (8.1%)
Class 6 (arcuate)	1 (2.7%)

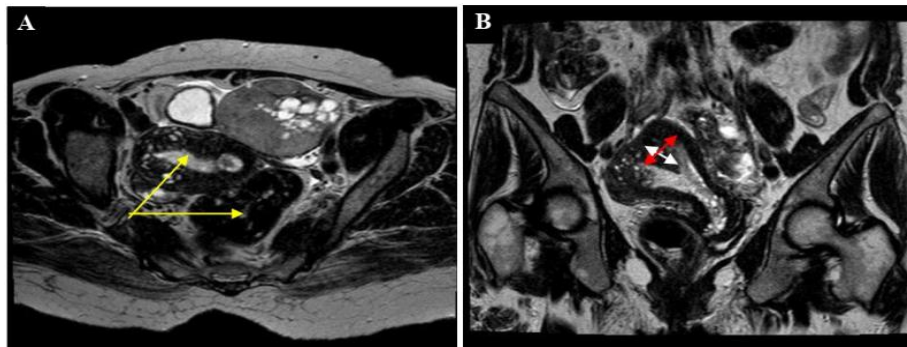
Other new classification is used to differentiate different uterine anomalies in our study which is ESHRE/ESGE classification. On application of the new classification of ESHRE/ESGE, 2/37 cases were class U0 (normal), 9/37 cases were class U1 (dysmorphic), 3/37 cases were U2 (septate), 13/37 cases were U3 (bicorporal), 2/37 cases were U4 (hemi-uterus), 5/37 cases were U5 (aplastic). 17/37 cases were C0 (normal cervix), 8/37 cases were C2 (double) and 12/37 cases were aplastic cervix. 16/37 cases were V0 (normal vagina), 1 case was V1 (longitudinal non obstructing vaginal septum), 5 cases were V2 (longitudinal obstructing vaginal septum), 3 cases were V3 (transverse vaginal septum) and 12 cases were V4 (aplastic vagina) as demonstrated in table (6).

Table (6): Classification of the Mullerian duct anomalies according to ESHRE/ESGE classification.

ESHRE/ESGE	The study group (n=37)
Uterus	
0 (normal)	2 (5.4%)
1 (dysmorphic)	9 (24.3%)
2 (septate)	3 (8.1%)
3 (bicorporal)	13 (35.1%)
4 (hemi-uterus)	2 (5.4%)
5 (aplastic)	8 (21.6%)
Cervix	
0 (normal)	17 (45.9%)
2 (double)	8 (21.6%)
4 (aplastic)	12 (32.4%)
Vagina	
0 (normal)	16 (43.2%)
1 (longitudinal non obstructing vaginal septum)	1 (2.7%)
2 (longitudinal obstructing vaginal septum)	5 (13.5%)
3 (transverse vaginal septum)	3 (8.1%)
4 (aplastic)	12 (32.4%)

**CASE PRESENTATION**

**Case 1:**



**Fig. (1):** 58 year old female had history of vaginal bleeding of 2 months duration ultrasound showed double uterus and a large left adnexal lesion. (A) Axial T2W image shows two uterine cavities (yellow arrows), the right cavity is of homogenous endometrium, and the left cavity is of low single endometrium (B) Coronal T2 image shows single cervix, the vertical fundal cleft measures 3 cm (white arrow) and the intercornual distance measures 6.7 cm (red arrow), The diagnosis is **bicornuate uterus**. This case is **class 4** according to AFS/ASRM classification and **U3C0V0** according to ESHRE/ESGE classification (arrow).

**Case 2:**

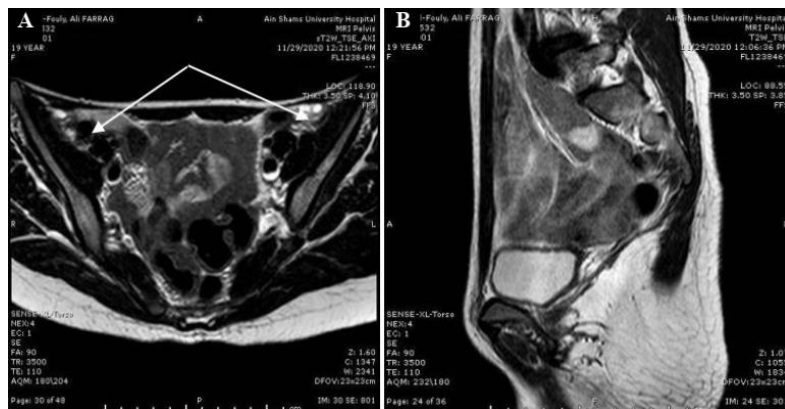


**Fig. (2):** 20 year old female had primary amenorrhea. There was no uterus by ultrasound. (A) Axial T2W and (B) sagittal T2W images show non visualized uterus, fallopian tubes and upper 2/3 of vaginal. The lower 1/3 of vagina was hypoplastic. Both ovaries were seen with multiple cysts (white arrows). **Mullerian agenesis or Mayer-Rokitansky-Küster-Hauser (MRKH) syndrome**, which is class 1 according to AFS/ASRM, **U5C4V4** according to ESHRE/ESGE classification.

**Case 3:**

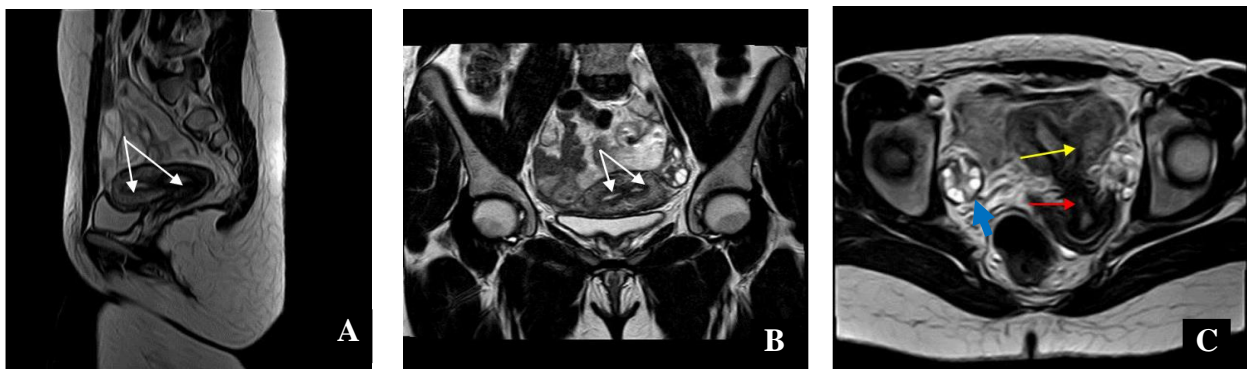


**Fig. (3):** 21 year old female had no symptoms. Suspected septate uterus was detected by ultrasound. (A) Sagittal T2W, (B) coronal T2 and (C) axial T1 images show normal-sized uterus with two endometrial cavities (white arrows). A septum is noted in the fundus separating two endometrial cavities. The upper part of septum (yellow arrow) is myometrium (intermediate T2 signal intensity), while the lower part is fibrous (low signal) (red arrow), which is partially extended to the

cervix. Normal endometrium, myometrium and junctional zone thickness is noted. Both ovaries are also enlarged with multiple small cysts (blue arrow). So, the diagnosis is septate uterus class 5 AFS/ASRM and U2C0V0 according to ESHRE/ESGE classification. The case is also associated with bilateral polycystic ovaries.

---

## DISCUSSION:

Congenital conditions known as Müllerian duct abnormalities (MDAs) are caused on by a failure of resorption, lateral or vertical fusion, or non-development of the Mullerian (paramesonephric) ducts<sup>(10)</sup>. Integrating clinical data with the use of several imaging modalities yields crucial indicators for the diagnosis of MDAs<sup>(11)</sup>. Imaging is used to identify and discriminate between Mullerian duct abnormalities that can be operated on and those that cannot<sup>(12)</sup>.

Due to its superior anatomical delineation, magnetic resonance imaging (MRI) has emerged as the mainstay imaging modality for the diagnosis and categorization of Müllerian duct abnormalities (MDA). For a number of diseases, including primary amenorrhea, infertility, or a poor obstetric history with regard to MDA, a pelvic MRI is recommended because it is crucial to determine the precise aetiology for these conditions<sup>(13)</sup>. Furusato-Hunt et al reported that magnetic resonance (MR) imaging is the best choice in diagnosis of MDAs due to its high accuracy, detailed delineation of the uterovaginal anatomy, non-invasiveness, and lack of ionizing radiation<sup>(14)</sup>.

Our study was performed in attempt to review MRI features of Mullerian Duct Anomalies and to classify them according to ASRM and ESHRE-ESGE classifications, guiding the future surgical management and minimizing the need for invasive diagnostic procedures such as laparoscopy and hysteroscopy making them restricted to difficult inconclusive cases. Our study group ages ranged from 6 to 58 years old with a mean age of 23.19 years. Forty-eight percent (48.6%) of them are aged from 20-30 years old. Female who aged <20 years were (32.4%) and those who aged >30 years old were (19.0%). This agreed with *Yousef et*

*al.*<sup>(12)</sup> who reported that MDAs are commonly diagnosed in the third decade.

*Heinonen et al.*<sup>(15)</sup> reported that, MDAs are usually asymptomatic unless an obstruction is present. The most common clinical presentation of MDAs is primary amenorrhea<sup>(15)</sup>. In our study, the most common symptom was primary amenorrhea. Out of the 37 cases, 17/37 (45.9%) cases presented with primary amenorrhea, 4/37 (10.8%) cases presented with infertility, 3/37 (8.1%) cases presented with abdominal pain, and only one patient (2.7%) presented with vaginal bleeding. Nine of thirty-seven (24.3%) patients in our study were asymptomatic.

In our study T1 and T2 images were used. This agreed with *Behr et al.*<sup>(16)</sup> who reported that T1 and T2 weighted sequences are required. They were very important in our study to reveal the three distinct intensities of the uterus which are the endometrium (high signal intensity), the junctional zone (low signal intensity) and the endometrium (intermediate signal intensity). The T1W images are important to describe the anatomy and help in diagnosis of the nature of any fluid collection or any associated gynaecological lesion. The coronal T1W sequence through the uterine fundus is the best for evaluating the fundal contour<sup>(17)</sup>.

*Pan et al.*<sup>(6)</sup> reported in their study that uterine agenesis was the most common type of MDA. This result goes in agreement with our study where uterine agenesis is the most common type (43.2%).

*Mooren et al.*<sup>(18)</sup> found that the most common congenital renal abnormality was unilateral renal agenesis, which was reported in almost two-thirds of his cases, but, in our

study, only one case has left renal agenesis (2.7% of all patients).

**Jegannathan et al.**<sup>(19)</sup> reported that ASRM classification does not specify classes for either obstructive cervical or vaginal malformations with normal uterus. It grouped them all under class I. This result goes in agreement with our study where ASRM classification failed to diagnose 2 cases (5.4%), with transverse vaginal septum.

**Ludwin et al.**<sup>(20)</sup> Independent classification of uterine, cervical and vaginal anomalies is made in ESHRE/ESGE. It is very useful, especially in cases of obstructive cervical or vaginal malformations with a normal uterus, which agree with our study in which all cases diagnosed using ESHRE/ESGE classification.

#### Conclusion:

MRI is an extremely useful imaging modality for assessment of female genital abnormalities as it provides reliably the vital imaging characteristics for the precise identification of Mullerian malformations. In addition, accompanying pelvic disease and any related renal abnormalities may be thoroughly assessed by MRI in a single scan, eliminating the requisite for supplementary diagnostic procedures.

#### Conflicts of Interest:

The authors state that the publishing of this paper is free of any conflicts of interest.

---

#### REFERENCES:

1. **Sugi MD, Penna R, Jha P, Pöder L, Behr SC, Courtier J, & Choi HH.** Müllerian Duct Anomalies: Role in Fertility and Pregnancy. *RadioGraphics* 2021, 41(6): 1857-1875.
2. **Castrillon DH.** Development and Maldevelopment of the Female Reproductive System. In *Gynecologic and Obstetric Pathology*. Springer, Singapore 2019; 1: 1-40.
3. **Pitot MA, Bookwalter CA, & Dudiak KM.** Müllerian duct anomalies coincident with endometriosis: a review. *Abdominal Radiology* 2020; 45(6): 1723-1740.
4. **Salwa MO, Sayed AS, & Elsayed Z.** Prevalence of congenital anomalies of uterus in Sohag Government: A descriptive study by trans-vaginal three dimensional ultrasound. *The Medical Journal of Cairo University* 2019; 87(December): 4645-4650.
5. **Acharya PT, Ponrartana S, Lai L, Vasquez E, & Goodarzian F.** Imaging of congenital genitourinary anomalies. *Pediatric radiology* 2021; 1-14.
6. **Pan HX, Liu P, Duan H, Li PF, Chen RL, Tang L, Luo GN, Chen CL.** Using 3D MRI can potentially enhance the ability of trained surgeons to more precisely diagnose Mullerian duct anomalies compared to MR alone. *European Journal of Obstetrics & Gynecology and Reproductive Biology* 2018; 228:313-8.
7. **Konrad L, Dietze R, Kudipudi PK, Horné F, Meinhold-Heerlein I.** Endometriosis in MRKH cases as a proof for the coelomic metaplasia hypothesis? *Reproduction*. 2019; 158(2): R41-7.
8. **Porter MB and Goldstein S.** Pelvic Imaging in Reproductive Endocrinology. In *Yen and Jaffe's Reproductive Endocrinology*. Elsevier 2019; 916-961.
9. **Ouyang Y, Yi Y, Gong F, Lin G, Li X.** ESHRE-ESGE versus ASRM classification in the diagnosis of septate uterus: a retrospective study. *Archives of Gynecology and Obstetrics*. 2018; 298(4):845-50.
10. **Junqueira BL, Allen LM, Spitzer RF, Lucco KL, Babyn PS, Doria AS.** Müllerian duct anomalies and mimics in children and adolescents: correlative intraoperative assessment with clinical imaging. *Radiographics*. 2009; 29(4):1085-103.
11. **Yoo RE, Cho JY, Kim SY, Kim SH.** A systematic approach to the magnetic resonance imaging-based differential diagnosis of congenital Müllerian duct anomalies and their mimics. *Abdominal imaging* 2015; 40(1):192-206.



12. **Yousef AF, Khater HM, Hussein IA.** Imaging of Müllerian duct anomalies. *Benha Medical Journal.* 2018; 35(2):194.
13. **Jegannathan D, Indiran V.** Magnetic resonance imaging of classified and unclassified Müllerian duct anomalies: Comparison of the American Society for Reproductive Medicine and the European Society of Human Reproduction and Embryology classifications. *SA Journal of Radiology* 2018; 22(1):1-3.
14. **Furusato-Hunt O, Li T, Hasan U, Myers RA, Sadowsky D, Rashid T, Gerard P.** Embryology Simplified: Using clay models as a novel teaching tool to aid in the visualization and understanding of reproductive and urinary embryology and their associated congenital disorders. *European Congress of Radiology-ECR* 2019.
15. **Heinonen PK.** Renal tract malformations associated with mullerian duct anomalies. *Clinical Obstetrics, Clin Obstet Gynecol Reprod Med,* 2018; 4(1): 1-5
16. **Behr, S. C., Courtier, J. L., & Qayyum, A. (2012):** Imaging of Müllerian duct anomalies. *Radiographics,* 32(6): E233-E250.
17. **Maciel C, Bharwani N, Kubik-Huch RA, Manganaro L, Otero-Garcia M, Nougaret S, Alt CD, Cunha TM, Forstner R.** MRI of female genital tract congenital anomalies: European Society of Urogenital Radiology (ESUR) guidelines. *European radiology.* 2020; 30(8):4272-83.
18. **Mooren ER, Cleypool CG, de Kort LM, Goverde AJ, Dik P.** A retrospective analysis of female müllerian duct anomalies in association with congenital renal abnormalities. *Journal of Pediatric and Adolescent Gynecology* 2021; 34(5):6815
19. **Jegannathan, D., & Indiran, V. (2018):** Magnetic resonance imaging of classified and unclassified Müllerian duct anomalies: Comparison of the American Society for Reproductive Medicine and the European Society of Human Reproduction and Embryology classifications. *SA Journal of Radiology,* 22(1): 1-13.
20. **Ludwin A and Pfeifer SM.** Reproductive surgery for müllerian anomalies: a review of progress in the last decade. *Fertility and Sterility* 2019; 112(3):408-16.

## المظهر التشريحي للأمراض الخلقية لقناه مولر عن طريق الرنين المغناطيسي

ياسمين ثروت السعيد ، نجلاء حسين شبريه ، سمر رمزي راغب

قسم الأشعة التشخيصية، كلية الطب - جامعة عين شمس- القاهرة-مصر.

**المقدمة:** تشكّل تشوهات مجرى مولر طيفاً معقداً من التشوهات التشريحية التي تنشأ من الانحرافات أثناء التطور الطبيعي لمجري مولر. في حالات الأطفال، لا يمكن أن يكون لمثل هذه الحالات أي أعراض قبل بداية سن البلوغ، ولكن يمكن أن ترتبط بأعراض انسداد أو تأثير ثانوي في حاله وجود القرن البدائي غير متصل أو حاجز مهلي عرضي. في بداية البلوغ، قد تعاني الفتيات المصابات بهذه الحالات من انقطاع الطمث الأولي، أو الانتباز البطني الرحمي، أو الحمل خارج الرحم، أو حالات الحمل الفاشلة المتكررة. تم أيضاً وصف تشوهات القناة المولارية بالاقتران مع مجموعة متنوعة من التشوهات الخلقية الأخرى. يعتبر التصوير بالرنين المغناطيسي أفضل طريقة لتقييم وتوصيف التشوهات في مجرى مولر لدى الأطفال بسبب طبيعتها غير الغازية، وقدراتها المتعددة، ونقص الإشعاع المؤين.

**هدف البحث:** هدفت هذه الدراسة إلى مراجعة ميزات التصوير بالرنين المغناطيسي لتشوهات مجرى مولر وتصنيفها وفقاً لتصنيفات ASRM و ESHRE-ESGE.

**المرضي والمنهجية:** كانت الدراسة عبارة عن دراسة سلسلة حالة شملت ٣٧ مريضاً خضعوا لتصوير الحوض بالرنين المغناطيسي في قسم الأشعة "مستشفيات جامعة عين شمس" في القاهرة، مصر.

**النتائج:** في دراستنا، وجد أن نقص التنسج، وعدم التخلق، والانحلال الوراثي لديهم نفس النسبة (٦,٢١٪)، بينما الرحم ثنائي القرن (٥,١٣٪)، الحاجز (١,٨٪)، الحاجز المهلي أحادي القرن والعرضي كلها نسبة حدوث (٤,٥٪) والأقل شيوعاً هو الرحم المقوس بنسبة (٧,٢٪).

**الخلاصة:** التصوير بالرنين المغناطيسي هو أداة مفيدة للغاية لتقييم تشوهات الأعضاء التناسلية الأنثوية، وهو قادر على إظهار ميزات التصوير الرئيسية بشكل موثوق للتشخيص الصحيح لتشوهات مولر. بالإضافة إلى ذلك، يمكن أن يوفر التصوير بالرنين المغناطيسي معلومات أساسية في فحص واحد، وتقييم شامل للأمراض الحوض العرضية والتشوهات الكلوية المصاحبة التي قد تكون موجودة، مما يلغي الحاجة إلى مزيد من الاختبارات التشخيصية.